Matrix modeling and optimization calculation method for large scale integrated energy system

Mohsen Sadiqi[a,*], Mahmoud Samiei Moghaddam[a], Amin Hajizadeh[b]

[a]*Department of Electrical Engineering, Damghan Branch, Islamic Azad University, Damghan, Iran*

[b]*AAU ENERGY, Aalborg University, Esbjerg, Denmark*

(Communicated by Ehsan Kozegar)

Abstract

We-Energy (WE), as an important energy unit with full-duplex and multi-energy carriers in the integrated energy system (IES), uses the coupling matrix to connect the network-side and demand-side energy. However, the coupling matrix of WE is very hard to be formulated directly due to the complicated internal structure and the flexibility of the operation mode. This paper proposes a multi-step method for the modeling of WE. According to the method, the conversion process in the WE can be separated into several steps and the WE model can be built by coupling matrix in each step. Then, the WE model is extended by considering the renewable energy, location of storage, and different types of demand response. Because of the non-linearity caused by the dispatch factors, the computational complexity increases greatly for solving the optimal scheduling issue of the WE. In order to reduce the computational burden, the variable substitution is added to the proposed modeling method. The results of simulation cases are presented to demonstrate the performance of the proposed modeling and calculation method.

Keywords: Integrated energy system, matrix modeling, optimization.
2020 MSC: 78M50, 80M50

1 Introduction

Soft computing methods have a wide range of applications [12, 13, 14]. In recent, the increasing concern of energy shortage and environmental change has facilitated a reconsideration of the current energy system. To curb carbon emission and improve energy efficiency, the concept of an integrated energy system (IES) where different types of energy carriers are integrated was proposed [5, 9]. In contrast to electric power systems, the IES is more complicated and flexible. How to realize the fast and accurate calculation of IES planning schemes and optimal scheduling strategies has become an important subject of the IES research [19]. In this context, many optimization models of the IES were established for optimal planning schemes and scheduling strategies, for which one of the most important types is the model of energy unit. Therefore, it can be considered that the model of energy units like energy hub (EH) and We-Energy (WE) constitutes the foundation of the IES model research [6, 11, 17].

The research of the energy unit model consists of two main parts: modeling of coupling matrix and calculation of the optimal operating state. For the modeling of the matrix, a method for building the coupling matrix of a small-scale

---

*Corresponding author
Email addresses: `first.author@email.address` (Mohsen Sadiqi), `Samiei352@yahoo.com` (Mahmoud Samiei Moghaddam), `third.author@email.address` (Amin Hajizadeh)

trigeneration system was presented in [4]. The dispatch factors were replaced by utilizing the augmented variable in the modeling of the coupling matrix in [18]. To reduce the computing resources in the building of the coupling matrix, a simple modeling technique for the large-scale EH model with complex constitute was proposed in [23]. The coupling matrix of the WE, which can act both as an energy consumer and as an energy supplier, was formulated based on the model of EH in [15] and [16]. But the elements changing in the coupling matrix caused by the full-duplex characteristic were not considered in this kind of model. In fact, although the modeling methods in [4, 15, 16, 18, 23] can characterize bi-directional energy exchange, it is realized by re-modeling different operation modes and formulating different models. However, there are huge differences between different models, even causing the physical meaning of each parameter in the model to change during operational mode transitions. Therefore, the mentioned coupling matrix modeling methods cannot represent the operation of WE completely and uniformly and bring difficulties for optimal scheduling. In order to solve the above problems, reference [24] investigated a modeling method of WE on the basis of the Hadamard Product and the formulated coupling matrix can clearly express the dynamic features of inner devices and the full-duplex characteristic of WE. However, for a large-scale WE model with complex construction (more than one conversion between input energy and corresponding output energy), the following issues still exist: 1) The modeling approaches of coupling matrix are too complicated for large WE. Moreover, the integration of storage and demand response brings more complexity to the coupling matrix modeling due to the influences caused by different situations of storage and demand response cite16, 17, 18. 2) The matrix is highly coupled according to existing modeling methods. Due to the coupling characteristics of the matrix, any replacement of devices in WE may require the entire model to be rebuilt. Thus, the workload is greatly increased. 3) Existing modeling methods involve large-scale matrix calculation, especially inversion computing, which is difficult for large-scale WE models. Hence, a simple modeling approach is important for the large-scale WE with complex construction.

For the optimal operation state, the non-linear optimal issue of energy units is formulated due to the dispatch factors contained in the coupling matrices [7, 10, 21]. Furthermore, because of the characteristic of bi-directional energy exchange and the unique trading mechanism of WE, the optimal issue of WE is a mixed-integer non-linear programming (MINLP) problem [21, 24]. Therefore, the calculation of the optimal operation state is time-consuming, and it is difficult to guarantee globally optimal. How to avoid dealing with the MINLP issue during scheduling the operation of WE needs to be addressed. To address these issues, the multi-step modeling (MSM) method is proposed in order to reduce the difficulty of direct WE modeling. Meanwhile, in each calculation step, the variable substitution method based on the MSM approach is also presented to realize the linearization of the WE model. In this paper, the major contributions can be expressed as:

- By utilizing the proposed MSM method, all kinds of WE models can be built easily. Based on the structure of the WE, the WE model can be classified into two categories: the non-cascading WE (NCWE) model and cascading WE (CWE) model. In the NCWE, there is at most one energy conversion between each input energy and corresponding output energy; Accordingly, in the CWE, some kinds of input energies are converted more than once to corresponding output energies. Based on the proposed modeling method, the coupling matrix of the NCWE model is formulated. The CWE model is also separated into several NCWE models and built by multiplying the NCWE model at each step. Moreover, the WE model extends renewable energy sources, storage locations, and different types of demand responses.

- The model of the CWE can be highly decoupled by using the MSM method. After decoupling, the mathematical representation of different devices can be clearly found in the model. Compared with existing WE modeling methods, the update of the coupling matrix is less complicated when the devices are replaced.

- The computational process of the high dimensional matrix, which requires a lot of computing time and resources for formulating the coupling matrix, is avoided. Since the complexity of large-scale matrix computation, peculiarly inversion computing, is much higher than that of several simple matrices multiplication, the separation of the CWE model based on the proposed method is useful for reducing the computational complexity of problems such as optimal operation.

- The non-linearity of the NCWE model is eliminated according to variables substitution and the elimination of non-linearity is extended to the arbitrary CWE model and combined with the proposed MSM method. Based on the presented linearization method, the MINLP problem is avoided and the computation for the global optimum is simplified significantly.

This paper is organized as follows: The proposed MSM method of WE is presented in Section 2. Section 3 presents the model which is integrated with renewable energy, storage and demand response. The linearization of the WE model

is presented in Section 4. Several cases are introduced in Section 5 to show the effectiveness of proposed method in a simulated IES. Section 6 finally provides the conclusion of this paper.

2 The proposed MSM method of WE

2.1 Basic Definitions of the MSM Method

The graph theory idea is borrowed for expressing connections between devices to simplify the structure of WE. There are several definitions to relate the graph theory concept and the physical structure.

- Each branch presents the energy flow through the corresponding converter. Note that if there are more input or output ports than one for a converter like CHP, then each energy flow through the input and output port together is regarded as a branch.

- The node not only denotes each input terminal and output terminal of WE but also denotes the start point and end point of each branch.

- Just like Kirchhoff's law in the electricity system, for each node, the output energy is equal to the input energy. Based on the dispatch factors, the output energy is dispatched to other nodes.

- The formulated graph for the WE model is directed and all branches have reference directions.

- The branches can be of two types, one kind is described by solid lines and the other is described by dashed lines. The branches with solid lines mean that the direction of the branches is the same as the corresponding energy flow direction. Otherwise, the branches with dashed lines intend that the direction of branches is opposite to the direction of the corresponding energy flow.

It also should be noticed that the virtual node can be set in a graph. According to the virtual node, a node can be divided into two nodes connected by a single branch with a coefficient of one.

2.2 The Coupling Matrix of the NCWE Model

In general, the IES can be thought of as consisting of several WEs. As a full-duplex energy unit, multiple energy carriers are coupled in WE. During operation, WE has different modes, and energy flows have different directions. For example, WE may sell electricity and purchase gas simultaneously if the gas price is low but the electricity price is high, and vice versa.
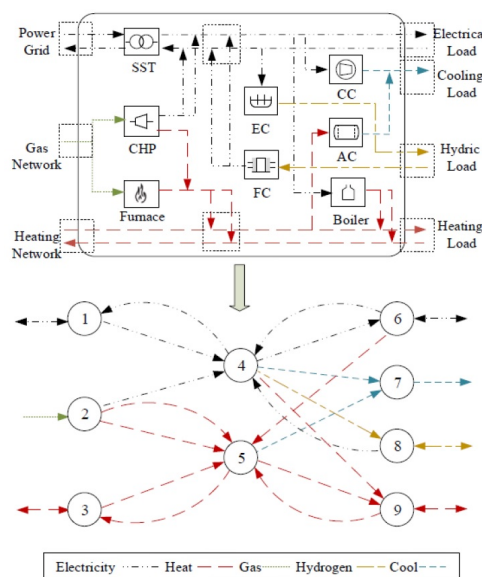
Figure 1: A type CWE model and the feasible energy flow.

The energy flow of NCWE can be expressed as:

$$DS_i = C_{ij} NS_j \tag{2.1}$$

where DS and NS represent energy flowing through demand side and network side, respectively. i and j are the index of nodes. The corresponding coupling matrix element is denoted by C_{ij}. Different from generally energy unit like EH, the values of DS_i and NS_j can be negative to show the working status of the WE. The parameters are negative mean corresponding nodes output energy. Otherwise, the nodes input energy if the parameters are positive. Since WE can purchase and sell energy simultaneously, the sign of each parameter is not required to be the same.

To represent the translation of operation mode and the dynamic property of the NCWE in full, C_{ij} can be denoted as:

$$C_{ij} = \sum_{l=1}^{N_l} v_{ij}^l \times n_{ij}^l + \sum_{\bar{l}=1}^{N_{\bar{l}}} \bar{v}_{ij}^{\bar{l}} \times \frac{1}{n^{\bar{l}}_{ij}} \tag{2.2}$$

where N_l and $N_{\bar{l}}$ are the number of parallel solid line branches and dashed line branches between node j and i, respectively. The forward dispatch factor for the energy flow from $j \longrightarrow i$ and converter efficiency are denoted by v_{ij} and n_{ij}. $\bar{v}_{ij}$ is the backward dispatch factor to describe the energy flow from $i \longrightarrow j$. For v_{ij} and $\bar{v}_{ij}$, it should be satisfied that

$$0 \le v_{ij} \le 1 \text{ and } 0 \le \bar{v}_{ij} \le 1 \tag{2.3}$$

$$\sum_{i=1}^{N_i} \sum_{l=1}^{N_l} v_{ij}^l + \sum_{i=1}^{N_i} \sum_{\bar{l}=1}^{N_{\bar{l}}} \bar{v}_{ij}^{\bar{l}} = 1 \tag{2.4}$$

where N_i is the number of nodes in corresponding node cluster. $\bar{v}_{ij}$ indicates the ratio of the energy, transmitted by the corresponding branch, to the total energy injected into the node j. It is clear that the physical meaning of $\bar{v}_{ij}$ is unlike common dispatch factor and all elements in the coupling matrix are directly represented. Moreover, no matter how operation mode changes, the physical meaning of the corresponding element will not be varied.
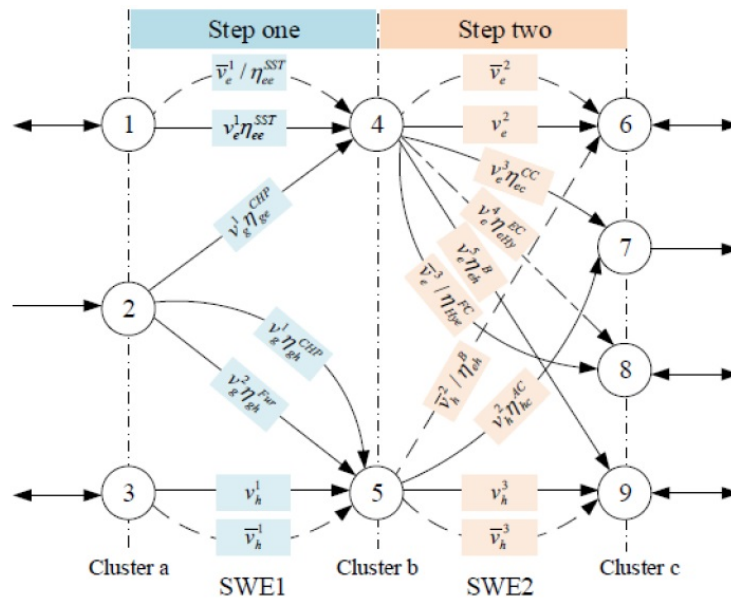
Figure 2: The directed weighted graph of CWE

2.3 The Coupling Matrix of the CWE Model

The coupling matrix of NCWE, where each energy is converted at most once, can be formulated according to (2.2). However, it is very common for energy to be processed several times and most of the WE models are CWE models in practice. It is also hard to establish a coupling matrix directly for the CWE model. A type of CWE and the feasible energy flow of the CWE model are shown in Fig. 1. The directed weighted graph of the model is shown in Fig. 2. The type CWE consists of a solid-state transformer (SST), an electrolytic cell (EC), a fuel cell (FC), a compression chiller (CC), an absorption chiller (AC), and a CHP, a furnace, and a boiler. Based on the internal devices, the CWE can process various kinds of energies and act both as an energy consumer and as an energy supplier. If each input energy is transformed the same number of times, then this CWE model can be directly divided into multiple NCWE models. From the perspective of the directed weighted graph, it can be concluded that the CWE model can be divided into several NCWE models directly if no branch through two or more stages. In the circumstances, an MSM method is proposed for dividing the conversion process into several steps. Moreover, the WE model in each step is an NCWE model whose coupling matrix can be formulated directly. Considering the CWE shown in Fig. 1 as a sample, the solution is represented as (2.5),(2.6),(2.7).

Step 1:

$$
\begin{pmatrix} P_4 \\ P_5 \end{pmatrix} = C_{s(1)} \begin{pmatrix} P_1 \\ P_2 \\ P_3 \end{pmatrix} = C_{s(1)} \begin{pmatrix} NS_e \\ NS_g \\ NS_h \end{pmatrix} = \left(\begin{pmatrix} v_e^1 \eta_{ee}^{SST} & v_G^1 \eta_{gh}^{CHP} & 0 \\ 0 & v_g^1 \eta_{ee}^{CHP} + v_G^2 \eta_{gh}^{Fur} & v_h^1 \end{pmatrix} + \begin{pmatrix} \frac{\bar{v}_e^1}{\eta_{ee}^{SST}} & 0 & 0 \\ 0 & 0 & \bar{v}_h^1 \end{pmatrix} \right) \begin{pmatrix} NS_e \\ NS_g \\ NS_h \end{pmatrix} \tag{2.5}
$$

Step 2:

$$
\begin{pmatrix} DS_e \\ DS_c \\ DS_{Hy} \\ DS_h \end{pmatrix} = \begin{pmatrix} P_6 \\ P_7 \\ P_8 \\ P_9 \end{pmatrix} = C_{s(2)} \begin{pmatrix} P_4 \\ P_5 \end{pmatrix} \left(\begin{pmatrix} v_e^2 & 0 \\ v_e^3 COP_{eE}^{cc} & v_H^2 COP_{hc}^{AC} \\ v_e^4 \eta_{eHy}^{EC} & 0 \\ v_e^5 \eta_{eh}^{Boiler} & v_h^3 \end{pmatrix} + \begin{pmatrix} \bar{v}_e^2 & \frac{\bar{v}_h^2}{\eta_{eh}^{Boiler}} \\ 0 & 0 \\ \frac{\bar{v}_e^3}{\eta_{Hye}^{FC}} & 0 \\ 0 & \bar{v}_h^3 \end{pmatrix} \right) \begin{pmatrix} P_4 \\ P_5 \end{pmatrix} \tag{2.6}
$$

Table 1: Detailed processing procedure for WE

Processing Content
Input: Directed graph $\mathcal{G}$ formulated by actual physical topology of WE:
(1) Arrange NS nodes to the initial group,
(2) Arrange DS nodes to the last group,
(3) **For** $\bar{n} = 1, 2, ...,$ **do**
(4) Calculate the branch number of maximum route r_{max} (from NS nodes to this node),
(5) Classify the node in to corresponding sequence of groups based on r_{max},
(6) **Until** $\bar{n}$ reach $N_{\bar{n}}$,
(7) **End for**
(8) **For** $\bar{b} = 1, 2, ...,$ **do**
(9) Acquire the sequence of star node ($\bar{S}$) and ending node ($\bar{E}$) for the branch,
(10) **If** $\bar{S} - \bar{E} > 1$
(11) Insert ($\bar{S} - \bar{E} - 1$) virtual nods into the branch,
(12) **End if**
(13) **Until** $\bar{b}$ reach $N_{\bar{b}}$,
(14) **End for**
(15) Recognize nodes form (1)-(7).
Output: Directed graph after processing $\mathcal{G}'$

The coupling matrix of the CWE can be described as:

$$
\begin{pmatrix} DS_e \\ DS_c \\ DS_{Hy} \\ DS_h \end{pmatrix} = C_{s(2)} \times C_{s(1)} \times \begin{pmatrix} NS_e \\ NS_g \\ NS_h \end{pmatrix} \tag{2.7}
$$

where $s(k)$ means step k. P_i is the power of node i. The number in the upper right corner of v and $\bar{v}$ represents the index of dispatch factor for corresponding energy. $\{e.h.c.g.Hy\}$ denote different kinds of energies such as electricity, heat, cooling, gas and hydrogen, respectively. Although WE can both get energy from the network and deliver it to the network. However, it is usually illogical for a certain kind of energy to be obtained from the network and delivered to the network at the same time. Thus, for $\forall\{i.j\} \in N_n$,

$$P_i v_{ij} \geq 0, \quad P_i \bar{v}_{ij} \geq 0 \tag{2.8}$$

where N_n is the number of nodes.

As mentioned above, the establishing condition for CWE which can be divided directly is too strict and not suitable for all kinds of CWE. Therefore, virtual nodes are introduced to make all WE model can utilize proposed MSM method. Defining the $N_{\bar{b}}$ and $N_{\bar{n}}$ represents the number of branches and nodes without NS and DS nodes, respectively. $\bar{b}$ and $\bar{n}$ are the index of branches and nodes except NS and DS nodes, respectively. The detailed procedure is shown in Table 1.

Remark 2.1. In contrast to the traditional energy unit model where energy flows in one direction, the WE model focuses on bidirectional energy flow and full duplex characteristics. For reverse energy flow, $P_j \bar{v}_{ij}^{\bar{l}}$ denotes how much power transmitted by branch $\bar{l}$ from node i to j. To calculate the output energy from node i, the reciprocal of corresponding converter efficiency $\frac{1}{\eta_{ij}^{\bar{l}}}$ is needed. The coupling matrix, which is formulated by proposed MSM, clearly represents the difference between WE and other energy units.

Remark 2.2. Virtual nodes is added in the branch that through two or more stages and one branch is divided into several branches which is connected by virtual nodes. Since there is no actual energy conversion, the weight of output branches for virtual nodes is 1.

3 The coupling matrix considering storage, renewable energy and demand response

3.1 Renewable energy and storage

Generally, renewable energy and multiple storages are contained in the WE model. The installation location of each device determines the position in the process of energy conversion, and all the devices can be installed at any position of WE [2, 22]. Therefore, to model the WE with different locations of renewable energy and storage uniformly, the devices are treated as extra inputs of the network side. According to the proposed MSM method, the WE model integrated with renewable energy and storage is denoted as:

$$DS^t = \begin{bmatrix} C^t & R^t & S^t \end{bmatrix} \begin{bmatrix} NS^t \\ P_{re}^t \\ Q_{out}^t - Q_{in}^t \end{bmatrix} \tag{3.1}$$

where R^t and S^t are coupling matrices for the renewable energy and the storage at time t, respectively. The matrices R and S can be formulated by utilizing the MSM method directly. P_{re} is the column vector of the renewable energy power. Similarly, the column vector of exchange powers for storages is denoted by $Q_{in/out}$. The stored energy SC at time t is described as:

$$SC_*^t = SC_*^{t-1}(1 - k_*) + (\eta_{s*}^+ Q_{out}^{t-1} - \frac{Q_{in}^{t-1}}{\eta_{s*}^-})\Delta T \tag{3.2}$$

where k is the loss rate factor of storage. Different types of storages are represented by $*$ and ΔT denotes a time slot. The storages should also be constrained by

$$0 \leq Q_{in}^t \leq \overline{Q_{in}} \quad 0 \leq Q_{out}^t \leq \overline{Q_{out}} \tag{3.3}$$

$$\underline{SC} \leq SC^t \leq \overline{SC} \quad 0 \leq P_{re} \leq \overline{P_{re}} \tag{3.4}$$

where $\overline{Q_{in}}$ and $\overline{Q_{out}}$ represent the column vectors of upper bounds on input power and output power, respectively. The column vectors of lower and upper bounds for storage content are denoted by $\underline{SC}$ and $\overline{SC}$ respectively. $\overline{P_{re}}$ is the column vector of the maximal renewable energy power.

3.2 Demand response

As an energy unit with high flexibility and close interaction with the network side, demand response is a non-negligible part during the operation of WE. Under the effect of prices or other incentives, the consumption behavior of WE can be changed. Therefore, the model of WE needs to be able to characterize the energy flow of the WE when performing demand response.

Compared with the electrical power system, the multiple energy demand responses of the IES have more types. Due to the presence of converters, the demand can be met according to the energy conversion [3]. Like the WE model shown in Fig. 1, the gas can be utilized to fulfill the electricity loads instead of electricity by using CHP. Moreover, some energy converters which belong to the consumer can also be used to satisfy demands [21]. On the other hand, the demands for different energy types can be shifted from one-time period to another [1].

For the first kind of demand response (FDR), the load on the demand side does not change. The essence of FDR is to use the flexibility of energy in WE to regulate the demand on the network side. The coupling matrix modeled in Section 2 can fully express the FDR of WE during operation.
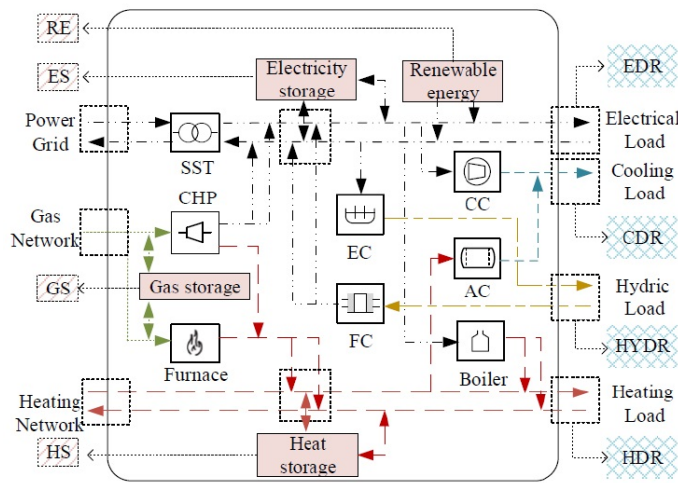
Figure 3: Type CWE with renewable energy, storages and demand response.

In the IES, the loads can be divided into critical loads and shiftable loads which can be reallocated during the operation. The purpose of the second kind of demand response (SDR) is to shift loads from the high-price time to the low-price time for decreasing the operation cost. The demand side powers after SDR can be described as:

$$DS^t = DS'^t - DR^t \tag{3.5}$$

where DS' and DR are the column vector of primary demand side powers and shifted loads, respectively. It should be noticed that the shifted loads in time t cannot exceed the total shiftable loads $DR^t \leq DR_{\max}$. Furthermore, the total load should be unchanged during an operating cycle $\sum_{t=1}^{N_t} DR^t = 0$. Combined with (3.1) and (3.5), the coupling matrix of WE extended with renewable energy, storages and demand response in time t is denoted as:

$$DS'^t - DR^t = \begin{bmatrix} C^t & R^t & S^t \end{bmatrix} \begin{bmatrix} NS^t \\ P_{re}^t \\ Q_{out}^t - Q_{in}^t \end{bmatrix} \tag{3.6}$$

A type CWE model considering renewable energy, three kinds of energy storages (electricity storage, heating storage and gas storage) and demand response for different loads are shown in Fig. 3. Storages and renewable energy are set as four extra input terminals. The demand response also impacts the energy supplied to the load side.

Remark 3.1. There is a special case in FDR that the energy is converted on the demand side. For this special case, an extra step can be extended in the WE model to formulate it based on the proposed modeling method.

4 Optimal scheduling model of we and solution method

4.1 Optimal Scheduling model of WE

As an important role in the IES, how to reach the optimal scheduling of WE is a crucial problem. Generally, the objective of WE operation is to achieve the minimal operating cost by dispatching the energy flows. Since the WE can be both energy consumer and energy supplier in IES, the objective function can be expressed as:

$$\min \ of: \ F = \sum_{t=1}^{N_t} \sum_{* \in N_e} (\theta_{t*} Pr_*^{buy} + (1 - \theta_{t*}) Pr_*^{sell}) NS_{t*} \tag{4.1}$$

where N_e represents all types of energy that WE interacts with network side. For each energy network, there is a price difference between the price at which energy is sold and the price at which energy is acquired. Thus, two different prices are shown in the (3.6) and Pr^{buy} and Pr^{sell} denote the price of buying energy and selling energy for WE, respectively. Furthermore, the judging factor θ is introduced to formulate the objective function. If $NS_{t*} \geq 0$, $\theta_{t*} = 1$, otherwise, $\theta_{t*} = 0$.

As shown in Section 2 and 3, the dispatch factors v_{ij} and $\bar{v}_{ij}$ are constrained in (2.3),(2.4) and remark 2.1. The renewable energy and storage are constrained in (3.2),(3.3),(3.4). The constraints for SDR are represented in Subsection 2.2 and the equality constraint of energy flow in WE is shown in (3.6). Combined with the constrains of judging factor θ and the objective shown in (4.1), the optimal operation model of WE based on the presented coupling matrix is formulated.

4.2 Linearization of the NCWE

According to the coupling matrix presented in (2.2), it can be noticed explicitly that the non-linearity is introduced by dispatch factors. The variable substitution method is a classical way which is widely used to eliminate the non-linearity [8]. Based on the formulated coupling matrix, the variable substitution method is involved to realize the linearization of WE model. A simple example can be shown as:

$$\begin{cases} P = Pv + P(1-v) & Pv \rightleftharpoons P' \\ 0 \leq v \leq 1 & P' \rightleftharpoons Pv \end{cases} \begin{cases} P = P' + (P - P') \\ 0 \leq P' \leq P \end{cases} \tag{4.2}$$

In the example, a single variable P', which can represent the input energy of corresponding converter, is introduced to substitute the product of two variables Pv. After the substitution, it can be noticed that the constraints are linearized. Moreover, the number of variables is not increased. Combined with (2.1) and (2.2), the model of NCWE can be denoted as:

$$NS_j \times \begin{cases} v_{ij}^l = P_{ij}'^l \\ \bar{v}_{ij}^l = \bar{P}_{ij}'^l \end{cases} \tag{4.3}$$

$$DS_i = \sum_{l=1}^{N_l} P_{ij}'^l \eta_{ij}^l + \sum_{\bar{l}=1}^{N_{\bar{l}}} \frac{\bar{P}_{ij}'^l}{\eta_{ij}^{\bar{l}}} \tag{4.4}$$

4.3 Linearization of the CWE

The NCWE model is linearized by utilizing the variable substitution method as shown in (4.2),(4.3),(4.4). However, due to the strong coupling caused by multiple energy conversions in CWE, this method is not suitable for directly eliminating the non-linearity of the CWE model. According to the previous study in Section 2, it is noticed that the model of CWE can be highly decoupled by utilizing proposed modeling method. Therefore, the method explained in (4.2) is expanded to the CWE by combining with proposed modeling method and can be expressed as:

$$\begin{cases} P'_{s(k-1)} = v_{s(k)} \circ P_{s(k-1)} \\ \bar{P}'_{s(k-1)} = \bar{v}_{s(k)} \circ P_{s(k-1)} \end{cases} \tag{4.5}$$

$$P_{s(k)} = f_{s(k)}(v_{s(k)} \cdot \bar{v}_{s(k)} \cdot P_{s(k-1)})$$
$$\downarrow$$
$$P_{s(k)} = f_{s(k)}(P'_{s(k-1)} \cdot \bar{P}'_{s(k-1)} \cdot P_{s(k-1)}) \tag{4.6}$$

where $k = 1...N_k \cdot v_{s(k)}$ and $\bar{v}$ are the vector of forward dispatch factor and backward dispatch factor in step k, respectively. The Hadamard product is denoted by $\circ$. As shown in Subsection 3.1, $P_{s(0)}$ is the power vector of nodes at step 0 which denotes the energy exchanges between WE and network side integrate with renewable energy and storage. It can be noted that $P_{s(0)} = [NS^t.P^t_{re}.Q^t]^T$, where $Q^t = Q^t_{out} - Q^t_{in}$. Similarly, from Subsection 3.2, the power vector of nodes at step N_k represents the demand side power after demand response. It can be expressed as:

$$P_{s(N_k)} = DS'^t - DR^t \tag{4.7}$$

As shown in (4.6), at each step k, the power of corresponding nodes for the CWE can be denoted by a linear function $f_{s(k)}$ with substitution variables and powers calculated in step $k - 1$. Therefore, a cluster of linear functions can replace the (3.6) and the constraints of energy flow in WE can be linearized based on the linearization method described above.

5 Numerical analysis

In this section, the proposed method is utilized for modeling and optimal scheduling a CWE which is designed on the basis of a real residential region in Changsha. The structure of the CWE is similar to the structure shown in Fig. 3. Based on the simulated model, five optimization scenarios are given and a computer with Intel Core i7 2.60 GHz CPU and 8 GB RAM is used to calculate the scenarios. The proposed method is solved by using Gurobi under MATLAB. The traditional method that formulates the MINLP is solved by using SCIP under MATLAB.

The efficiencies and capacities of devices in the CWE are shown in Table 2.

Table 2: Efficiencies and capacities of devices

Device	Capacity	Efficiency
SST	920kW	$\eta^{SST}_{ee} = 0.93$
CHP	390kW	$\eta^{CHP}_{ge} = 0.32 \cdot \eta^{CHP}_{gh} = 0.46$
Furnace	210kW	$\eta^{Fur}_{gh} = 0.92$
Electrolyte Cell	400Kw	$\eta^{EC}_{eHy} = 0.55$
Fuel Cell	280kW	$\eta^{FC}_{Hye} = 0.5$
Boiler	240kW	$\eta^{Boiler}_{eh} = 0.94$
Compression Chiller	120kW	$\eta^{CC}_{ec} = 2$
Absorption Chiller	130kW	$\eta^{AC}_{hc} = 1.2$

Table 3 shows the parameters of different storages. Table 4 denotes the buying prices (BP) and selling prices (SP) of different kinds of energies. The periods of prices are set as: 0:00-7:00 and 23:00-24:00 are Bottom hours; 7:00-9:00 and 19:00-23:00 are Flat hours; 9:00-19:00 are Peak hours. The demand side can supply hydrogen to the CWE. The maximum demand responses for electricity, heat, cooling and hydrogen loads are 80kW, 70kW, 50kW and 25kW, respectively.

Table 3: Parameters of different storages

Storage	Discharge (max)	Charge (max)	Storage Level (max/min)	Loss Rate
Electricity	210kW	170kW	320kWh/10kWh	5%
Heat	80kW	70kW	200kWh/5kWh	8%
Gas	200kW	200kW	500kWh/0kWh	0%

The data of loads and renewable energy adopts from a typical summer day are shown in Fig. 4. For the sake of demonstration, the units of all types of energy are converted to kWh.

Table 4: Energy prices on different periods

Load Periods	BP(e)/SP(e) (CNY/kWh)	BP(h)/SP(h) (CNY/kWh)	BP(g)/SP(g) (CNY/m^3)
Peak	1.009/0.892	0.48/0.892	4.39/3.83
Flat	0.687/0.452	0.48/0.452	4.39/3.83
Bottom	0.315/0.194	0.48/0.42	4.39/3.83
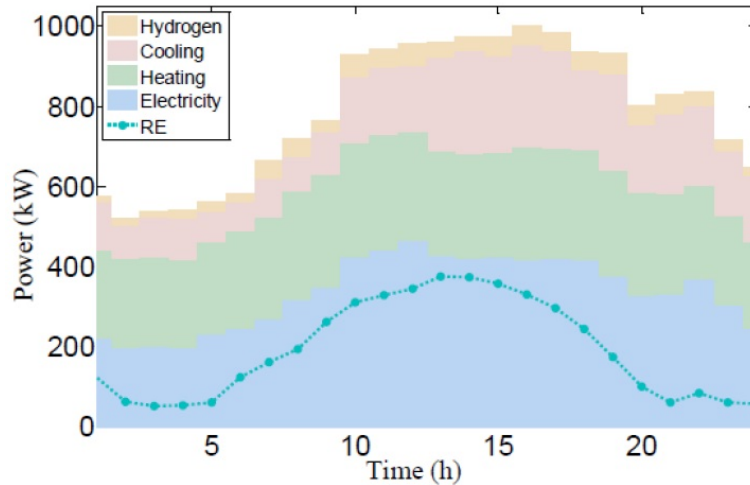
Figure 4: The demand and renewable energy.

5.1 Scenario 1: considering neither energy storages nor demand response

This scenario is formulated to show the operation of the CWE without considering energy storages and demand response. Fig. 5 shows the operation results of devices in the CWE and the energy transaction between CWE and the network side. Based on the characteristic of CWE, different energy types can complement each other and energy transactions between networks and devices are highly flexible, which can reduce the cost. From the figure, it can be clearly found that during 0:00-7:00, the boiler works and the furnace is inactive since it costs less to produce heat from boiler than from furnace. However, due to the changing of electricity prices, the operation cost of boiler is increased and the operating states of the two devices are switched during 9:00-23:00. As the operation results shown, the WE can sell and purchase different kinds of energies simultaneously. Thus, the full duplex characteristic of the WE can be noticed obviously.
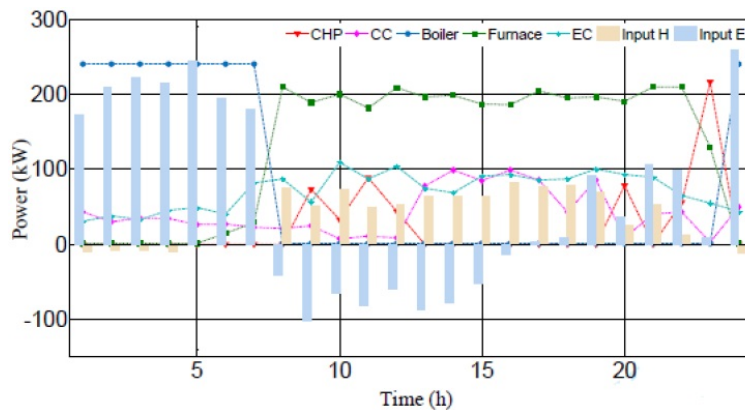
Figure 5: The operation result of different devices and energy transaction between CWE and networks for scenario 1.

5.2 Scenario 2: considering energy storages without demand response

As an important role in the IES, the energy storage devices have great effect on energy management of the system. The operation results are shown in Fig 6. With the utilization of energy storages, by using the price difference of energy

during the day, the operation cost can be reduced by charging and discharging the energy storage devices in different time periods. For example, the electricity energy storage device discharges all the stored energy during 10:0013:00 since the electricity price is high in that time period. It can also be found that storage devices, other than gas storage devices, do not store energy for long periods of time because of the energy loss rate of energy storage devices. Each storage device stores the same amount of energy at the beginning and end of the day, so as not to interfere with the schedule of next day. Moreover, due to the addition of energy storages, although the operation results of devices is similar to scenario 1, the operation cost decreases from 2724.3 CNY in scenario 1 to 2599.2 CNY in scenario 2.
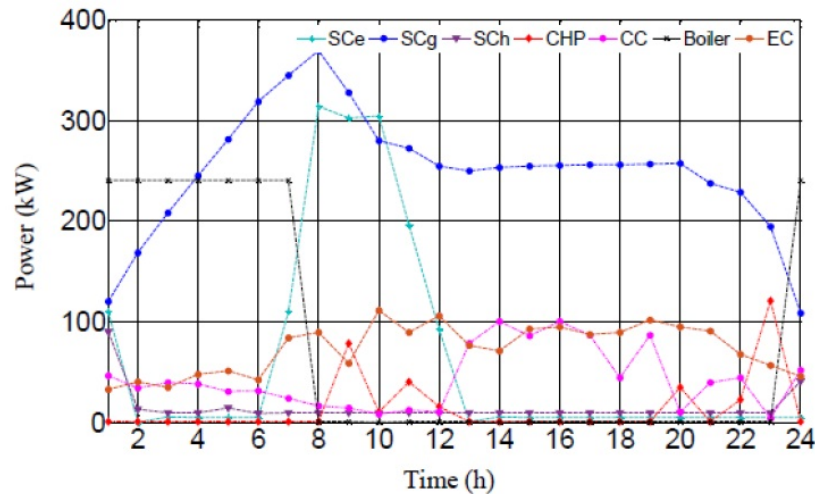
Figure 6: The stored energy of storages and operation of devices.

5.3 Scenario 3: considering demand response without energy storages

The demand response plays a vital role in peak shaving. Because of the mechanism of time-of-use pricing, the demand response can reduce the cost during operation. The change of loads before and after the implementation of demand response in a day are depicted in Fig. 7. According to the result, it can be seen that the demand response for cooling loads is used to shift the load from time periods (9:00-19:00 and 20:00-22:00) to another period (0:00-9:00). The main reason is that the electricity that can be used for cooling is more expensive during the time period 9:00-19:00. The electricity and heat loads are also shifted in the similar periods to reduce energy purchases when the prices are high. The operation cost in scenario 3 is 2016.3 CNY. Compared with scenario 1, the operation cost reduces about 26% because of the application of demand response.
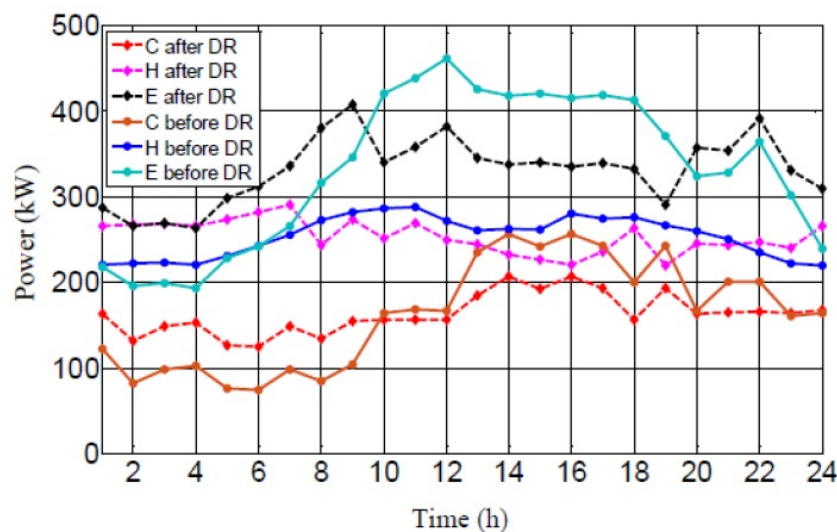
Figure 7: The change of loads before and after the implementation of demand response.

5.4 Scenario 4: considering both storages and demand response

The operation of deceives and energy transaction between CWE and networks for this scenario are shown in Fig. 8. Compared with Fig. 5 and Fig. 8, it can be clearly found that the CHP produce more power with the support of gas storage device and the cooling loads are almost supplied by AC after 9:00.
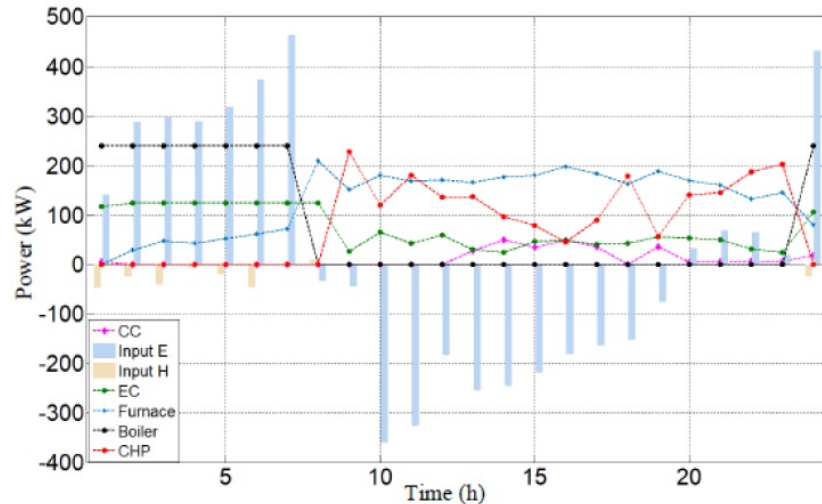
Figure 8: The operation result of different devices and energy transaction between CWE and networks for scenario 4.

With the utilization of demand response, the CC can be as inactive as possible to reduce the consumption of electricity since the cooling loads are shifted. Moreover, the transaction peaks in scenario 4 are much higher than those in scenario 1, whether buying or selling electricity. By using the demand response and storage devices, the CWE can buy more energy to satisfy loads or store it in storage devices when prices are low (0:007:00 and 23:00-24:00), and sell more energy when prices are high (9:00-19:00) to reduce operating cost. The cost in this scenario is 1890.6 CNY. Compared the operation cost in scenario 4 to those in scenario 3 and scenario 2, it can be noticed that the demand response and energy storage devices can cooperate with each other to reduce the cost of the CWE model during operation.

5.5 Scenario 5: large-scale model for five residential regions

The purpose of this scenario is to show the performance of the proposed method in a large-scale WE model. The WE model is consisted by five residential regions. There are five SSTs, five CHPs, five furnaces, five ECs, five CCs, five ACs, five FCs, five boilers, five energy load consumers, an electricity storage, a heat storage, a gas storage and a renewable energy device. The parameters of the converters are shown in Table 2. The maximum demand response for electricity, heat, cooling and hydrogen loads are 400kW, 350kW, 200kW and 125kW, respectively. The capacity of electricity storage, heat storage and gas storage are 920kWh, 700kWh and 1200kWh, respectively. Based on the model, scenario 1-4 was recalculated using two different methods in scenario 5.

Table 5 denotes the performance between proposed method and traditional non-linear solving method in different scenarios. In any scenarios, the proposed method saves at least 99% of the time. For scenarios 1-4 (small-scale WE), although the optimal value obtained by the proposed method is equal to that obtained by the traditional method, the computation time of the proposed method is much less than that of the traditional method. Compared with the calculation of small-scale model, the calculation time of the proposed method does not increase significantly in the calculation of large-scale WE model. However, the traditional method does not get the optimal value in the specified number of iterations, and the computation times increase by more than 10 times compared with the previous results.

6 Conclusion

An MSM method for WE has been proposed in the paper. Based on the method, the model of CWE can be separated into several NCWE models and the mathematical representation of different devices can be clearly found in the model. The separation of the CWE model can avoid the computational process of the high dimensional

Table 5: Performances between proposed method and traditional method

Scenario	Optimal Cost (CNY)		Calculation time (s)	
	Proposed Method	Non-Linear Method	Proposed Method	Non-Linear Method
1	2724.3	2724.3	0.1162	23.15
2	2599.2	2599.2	0.3309	61.21
3	2016.3	2016.3	0.1554	29.69
4	1896.3	1896.6	0.375	70.33
5.1	29534	29639	0.1241	716.91
5.2	29179	29464	0.3632	755.83
5.3	27968	28072	0.195	791.69
5.4	27485	28047	0.3943	822.09

matrix, which is useful for reducing the computational complexity of problems such as optimal operation. Moreover, the elimination of non-linearity has been extended to an arbitrary WE model combined with the proposed MSM method and the MINLP problem can be avoided. Therefore, the computation for global optimum has been simplified significantly. Five different scenarios are given in the simulation part to show the effectiveness of the proposed method. According to the results, it has been proved that the storage device and demand response are effective ways to reduce the operating cost. Furthermore, the proposed modeling and calculating method can reduce more than 99% computation time for achieving the global optimum.

References

[1] M. Alipour, K. Zare and M. Abapour, *MINLP probabilistic scheduling model for demand response programs integrated energy hubs*, IEEE Trans Ind. Inf. **14** (2018), no. 1, 79–88.

[2] M.H. Barmayoon, M. Fotuhi-Firuzabad, A. Rajabi-Ghahnavieh and M. Moeini Aghtaie, *Energy storage in renewable-based residential energy hubs*, IET Gener. Transm. Distrib. **10** (2016), no. 13, 3127–3134.

[3] F. Brahman, M. Honarmand and S. Jadid, *Optimal electrical and thermal energy management of a residential energy hub, integrating demand response and energy storage system*, Energy Build. **90** (2015), 65–75.

[4] G. Chicco and P. Mancarella, *Matrix modelling of small-scale trigeneration systems and application to operational optimization*, Energy **34** (2009), no. 3, 261–273.

[5] S. Clegg and P. Mancarella, *Integrated electrical and gas network flexibility assessment in low-carbon multi-energy systems*, IEEE Trans. Sustain. Energy. **7** (2016), no. 2, 718–731.

[6] M. Geidl, G. Koeppel, P. Favre-Perrod, B. Klockl, G. Andersson and K. Frohlich, *Energy hubs for the future*, IEEE Power Energy Mag. **5** (2007), no. 1, 24–30.

[7] J. Hinker, H. Knappe and J.M.A. Myrzik, *Precise assessment of technically feasible power vector interactions for arbitrary controllable multi-energy systems*, IEEE Trans. Smart Grid **10** (2019), no. 1, 1146–1155.

[8] Y. Li, H. Zhang and X. Liang, *Event-triggered based distributed cooperative energy management for multienergy systems*, IEEE Trans Ind. Inf. **15** (2019), no. 14, 2008–2022.

[9] K. Mahmud, B. Khan, J. Ravishankar, A. Ahmadi and P. Siano, *An internet of energy framework with distributed energy resources, prosumers and small-scale virtual power plants: An overview*, Renew. Sustain. Energy Rev. **127** (2020), 1–19.

[10] M. Moeini-Aghtaie, P. Dehghanian, M. Fotuhi-Firuzabad and A. Abbaspour, *Multiagent genetic algorithm: An online probabilistic view on economic dispatch of energy hubs constrained by wind availability*, IEEE Trans. Sustain. Energy **5** (2014), no. 2, 699–708.

[11] K. Orehounig, R. Evins and V. Dorer, *Integration of decentralized energy systems in neighbourhoods using the energy hub approach*, Appl. Energy **154** (2015), 277–289.

[12] A. Rahmani, J. Haddadnia and A. Sanai, *Intelligent detection of electrical equipment faults in the overhead substations-based machine vision*, 2nd Int. Conf. Mech. Electron. Engin., IEEE, **2** (2010), V2–141.

[13] O. Rahmani Seryasat, J. Haddadnia and H. Ghayoumi Zadeh, *Assessment of a novel computer aided mass diagnosis system in mammograms*, Iran. J. Breast Disease **9** (2016), no. 3, 31–41.

[14] H. Razavi, H. Sarabadani, A. Karimisefat and J.F. Lebraty, *Profitability prediction for ATM transactions using artificial neural networks: a data-driven analysis*, 5th Conf. Knowledge Based Engin. Innov. (KBEI), IEEE, 2019, pp. 661–665.

[15] Q. Sun, *Energy internet and we-energy*, Berlin, Germany: Springer, 2018.

[16] Q. Sun, R. Fan, Y. Li, B. Huang and D. Ma, *A distributed double-consensus algorithm for residential we-energy*, IEEE Trans. Ind. Inf. **15** (2019), no. 8, 4830–4842.

[17] Q. Sun and L. Yang, *From independence to interconnection–A review of AI technology applied in energy systems*, CSEE J. Power Energy Syst. **5** (2019), no. 1, 21–34.

[18] Y. Wang, J. Cheng, N. Zhang, and C. Kang, *Automatic and linearized modeling of energy hub and its flexibility analysis*, Appl. Energy **211** (2018), 705–714.

[19] D. Wang, L. Liu, H. Jia, W. Wang, Y. Zhi, Z. Meng and B. Zhou, *Review of key problems related to integrated energy distribution systems*, CSEE J. Power Energy Syst. **4** (2018), no. 2, 130–145.

[20] Y. Wang, N. Zhang, C. Kang, D.S. Kirschen, J. Yang and Q. Xia, *Standardized matrix modeling of multiple energy systems*, IEEE Trans. Smart Grid **10** (2019), no. 1, 257–270.

[21] L. Yang, Q. Sun, D. Ma and Q. Wei, *Nash Q-learning based equilibrium transfer for integrated energy management game with we-energy*, Neurocomput. **396** (2019), 216–223.

[22] M. Zarif, S. Khaleghi and M.H. Javidi, *Assessment of electricity price uncertainty impact on the operation of multi-carrier energy systems*, IET Gener. Transm. Distrib. **9** (2015), no. 16, 2586–2592.

[23] D. Zhang and T. Liu, *A multi-step modeling and optimal operation calculation method for large-scale energy hub model considering two types demand responses*, IEEE Trans. Smart Grid **10** (2019), no. 6, 6735–6746.

[24] N. Zhang, Q. Sun and L. Yang, *A two-stage multi-objective optimal scheduling in the integrated energy system with we-energy modeling*, Energy **205** (2020).